Multivariable Sensors

DOI: 10.1002/anie.201305303

Detection of Individual Vapors and Their Mixtures Using a Selectivity-Tunable Three-Dimensional Network of Plasmonic Nanoparticles**

Radislav A. Potyrailo, Michael Larsen, and Orrie Riccobono*

Vapor detection is needed in a variety of applications, ranging from environmental monitoring, to industrial safety, medical diagnostics, and homeland security.[1] Sensors with a sensing material applied onto a physical transducer, have operational advantages over other detectors that include continuous detection, little or no power consumption, unobtrusive form factors, and no consumables.[2] However, poor selectivity of individual sensors is one of their key problems.[3] Combining individual sensors into arrays[4] became an accepted approach to improve selectivity, for example, as shown in recent excellent reports.[5] Unfortunately, sensor arrays suffer from problems with unknown interferences, uncorrelated noise from individual sensors, and heterogeneous aging of sensing materials.

Thus, development of selectivity-tunable yet simplified sensor systems attracts tremendous attention.[6] Our and other research teams are developing new concepts of chemical detection with multivariable sensors, where an individual sensor has several partially or fully independent responses. Such single sensor has several advantages over sensor arrays that include a reduced number of noise sources, more predictable sensor aging, and simplified fabrication/packaging. Examples of such sensors include electrical and mechanical resonators, field-effect transistors, and optical sensors based on quantum dots, multi-reporter fluorophores, biological iridescent nanostructures, core–shell nanoparticles, and plasmonic metal/metal-oxide nanocomposites.[7]

In this study, we achieved selective detection of not only individual vapors but also their mixtures using a single sensing material and its localized surface plasmon resonance (LSPR) spectroscopic readout. While LSPR detection of individual vapors has been shown with plasmonic nanoparticles,[7i,8] here we demonstrate detection of vapor mixtures with a single LSPR sensing film. To achieve this attractive capability, instead of using a two-dimensional (2D) arrangement of surface-attached plasmonic nanoparticles,[7i,8a–c,e] we implemented a 3D network of dispersed plasmonic nanoparticles functionalized with a "soft" vapor-sorbing ligand shell and coupled its LSPR response with multivariate spectral analysis. Earlier, such monolayer-functionalized metal nanoparticles were used for sensing with univariate transducers,[8d,9] but required sensor arrays with diverse vapor-sorbing ligands for vapor-response selectivity.[5b,d,9c,10]

The three mechanisms facilitating the vapor response selectivity of LSPR sensors reported in this study are illustrated in Figure 1 A. First, the swelling/shrinking of the soft shell is affected by the type and concentration of the vapor, resulting in the change in the interparticle spacing D.[11] Second, vapors have their respective vapor partition coefficients K into the organic vapor-sorbing ligand shell[5d,9c] that affect the resulting dielectric constant of the shell ε_r, which is in turn related to its refractive index n. Third, reflectivity R of the metal nanoparticle network films is affected by the variations of the film thickness.[11a,12] These diverse effects

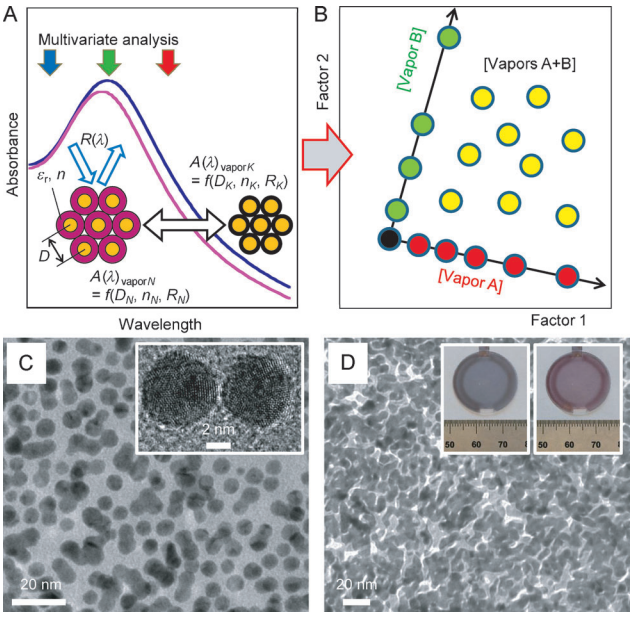

Figure 1. Selective detection of vapors using a single sensing film based on a 3D network of organothiol-functionalized plasmonic nanoparticles: A) Mechanisms facilitating vapor response selectivity involve vapor-induced modulation of interparticle spacing D, dielectric constant ε_r, and refractive index n of the ligand shell, and film reflectivity R. B) Concept of spectral discrimination of vapors A and B and their mixtures A + B upon multivariate analysis of resulting LSPR spectra. C) TEM image of 1-mercapto-(triethylene glycol) methyl ether functionalized gold nanoparticles. Inset, high-resolution TEM of two nanoparticles. D) TEM image of a sensing film formed from nanoparticles. Insets, color change of the spin-cast sensing film before (left) and during (right) water vapor exposure.

[*] Dr. R. A. Potyrailo, M. Larsen, O. Riccobono
GE Global Research Center, Niskayuna, NY 12309 (USA)
E-mail: potyrailo@crd.ge.com

[**] We thank M. Pietrzykowski, W. P. Hall, M. Palacios, J. Grande, and Z. Tang for useful discussions. This work was supported by US ARO, contract number W911NF-10-C-0069 and by GE's Advanced Technology Program. The views and conclusions contained here are those of the authors and should not be interpreted as presenting the official policies or position of US ARO or the US Government.

Supporting information for this article is available on the WWW under http://dx.doi.org/10.1002/anie.201305303.

provide the possibility to spectrally discriminate different vapors and their mixtures upon multivariate analysis of resulting LSPR spectra and an attractive opportunity to quantify individual vapors in their mixtures using only a single LSPR film (see Figure 1B). Depending on the nature of the ligand shell, type, and concentration of the vapor, morphology and thickness of the formed nanoparticle network film, and measurement conditions, the relative contributions from the various mechanisms of the vapor-induced film response can differently affect vapor selectivity of a single film.

Out of a variety of soft ligand shells,[6b] we selected 1-mercapto-(triethylene glycol) methyl ether for functionalization of gold nanoparticles because of its amphiphilic properties that provide the ability to respond to both polar and nonpolar vapors as well as the strong color change upon vapor exposures. Individual nanoparticles, the spin-cast sensing film, and its color change upon vapor exposure (water vapor, at a concentration of about 0.8 P/P_0, where P is the vapor partial pressure and P_0 is the saturated vapor pressure) are visualized in Figure 1C,D. A transmission electron microscopy (TEM) image in Figure 1C illustrates that the nanoparticles are 6.0 ± 0.8 nm in diameter (mean $\pm$ standard deviation, SD). The formed 3D network[13] is a random dispersion of nanoparticles with visible voids (Figure 1D). These voids (also known as "regions of lower ligand density"[9a]) facilitate rapid diffusion of vapors into and out of the film. Spin-casting or printing of such sensing films could be an advantage over monolayer films because of the simplicity of their fabrication, yet providing excellent performance.[5b,d]

As model vapors, we selected six vapors (water, methyl salicylate, tetrahydrofuran, dimethylformamide, ethyl acetate, and benzene) with diverse range of their physical and chemical properties and importance for industrial and homeland protection applications (see Table S1 in the Supporting Information). Absorption spectra of the sensing film upon exposure to six vapors are presented in Figure S1. The plasmonic response at the short- and long-wavelength shoulders showed a significant diversity to different vapors. Irrespective to their refractive index (see Table S1), all vapors have led to the peak shift toward short wavelengths, indicating noticeable contributions of swelling effects of the organic soft shell upon interactions with vapors of different refractive indices.

Exposures to different vapors at several concentrations were further performed to evaluate the response pattern. For this assessment, we selected several wavelengths, including those at the short- and long-wavelength shoulders of the extinction peak and at the peak maximum (see Figure 2 and Figure S1). Different vapors had their varying response and recovery times ranging from the relatively fast (for water, ethyl acetate, benzene) to the relatively slow (for methyl salicylate). For each vapor, these dynamic responses were the same at different wavelengths of the spectrum.

From the evaluation of the responses at individual wavelengths, we observed that tested vapors had different relative magnitudes and even directions of response. Figure 3A summarizes these response intensities at several representative wavelengths (440, 510, and 610 nm) normalized by the response of a representative vapor (vapor 3). To explore in

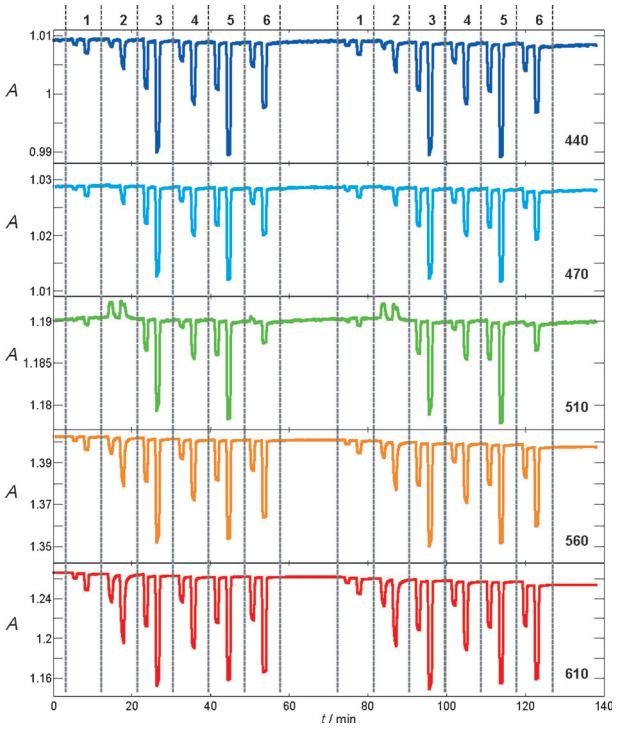

Figure 2. Dynamic response patterns of a single sensing film of organothiol-functionalized plasmonic nanoparticles to six model vapors at representative wavelengths (440, 470, 510, 560, and 610 nm). Vapors: 1) water, 2) methyl salicylate, 3) tetrahydrofuran, 4) dimethylformamide, 5) ethyl acetate, and 6) benzene. All vapors are at 0.09 and 0.18 P/P_0.

detail the effects of different vapors on the absorption spectra of the sensing film, we analyzed spectra using principal components analysis (PCA).[14] This pattern recognition method explains the variance of the data as the weighted sums of the original variables, known as principal components (PCs). Figure 3B depicts the scores plot of PC_1 versus PC_2 upon exposure of the single sensing film to six vapors. The first two PCs of the built PCA model accounted for $>99\,\%$ of the total variance. This single sensing film discriminated between most of the tested vapors as shown with replicate measurements ($n=2$). The response of the film to water vapor was close to the response to tetrahydrofuran and dimethylformamide at tested concentrations. A slight response nonlinearity was observed for methyl salicylate and tetrahydrofuran.

We have found that the order of the response of the sensing film to different vapors in the PCA scores plot corresponded to the refractive index of the solvent (dashed line in Figure 3B). Almost all tested vapors followed this ranking except for water vapor. Such behavior of the sensing film upon exposure to water vapor could be preliminary explained that water was the only polar protic solvent among tested vapors. This response behavior is currently under our detailed evaluation. Such diversity of vapor responses is a significant improvement in design of sensing materials where selectivity is achieved by the multivariate response of an individual film. Selectivity tuning can be achieved not only by diverse functionality of soft vapor-sorbing ligands, but also

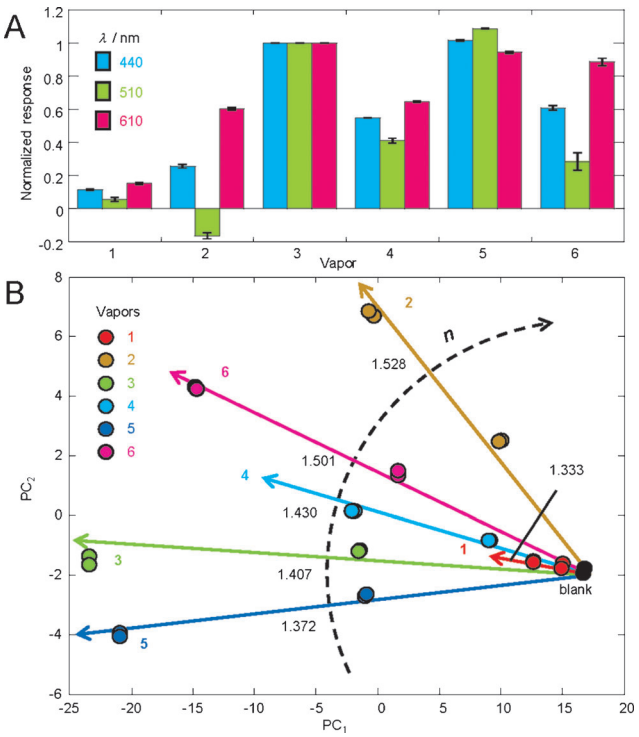

Figure 3. Discrimination of six individual vapors using a single sensing film of organothiol-functionalized plasmonic nanoparticles: A) Univariate responses at representative wavelengths (440, 510, and 610 nm) normalized by the response to vapor 3. Each data point is the mean of two replicate exposures, error bars are ±1 SD. B) Scores plot of a developed PCA model. Each vapor concentration is represented by two replicate exposures. The dashed line shows the film response to different vapors in the order of the refractive indices *n* of the corresponding solvent. Vapors: 1) water, 2) methyl salicylate, 3) tetrahydrofuran, 4) dimethylformamide, 5) ethyl acetate, and 6) benzene. All vapors are at A) 0.36 and B) 0.09 and 0.18 P/P_0.

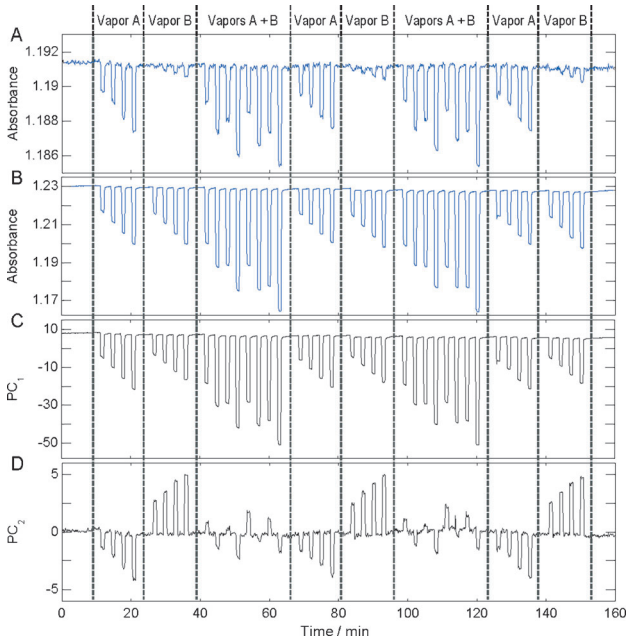

Figure 4. Detection of individual vapors A (ethyl acetate) and B (benzene) and their binary mixtures using a single sensing film of organothiol-functionalized plasmonic nanoparticles: A,B) Film absorbance at 510 and 610 nm, respectively. C,D) Responses PC_1 and PC_2, respectively from a built PCA model.

by implementing more rigid vapor-sorbing ligands that restrain swelling of sensing films and boost the effects of analyte-dependent changes of the dielectric constant and the refractive index of the film.[6b]

Selectivity for diverse classes of vapors (Table S1) reported in this study, has not been previously observed in photonic sensing structures. In particular, 2D arrays of surface-immobilized plasmonic nanoparticles decorated with vapor-responsive layers (e.g. metal–organic frameworks,[8c] metal oxides[7i,8e]) did not show such selectivity. Nanofabricated sensors based on Bragg diffraction (e.g. porous silicon, opal structures, inverse opal structures, and periodic layers of SiO_2 and TiO_2 nanoparticles[15]) did not discriminate different vapors within a chemically uniform photonic layer.[16]

For studies of sensor response to binary vapor mixtures, we identified ethyl acetate and benzene vapors (vapors A and B, respectively) based on the PCA scores plot in response to six vapors (Figure 3B). These vapors were selected because of their good separation in the scores plot in Figure 3B, rapid response/recovery times, and significant differences in their dielectric properties and refractive index (see Table S1).

The sensing film was exposed to pure vapors at different concentrations, followed by the exposure of the sensor to eight mixtures of vapors A and B at their different ratios. Figure S2 depicts the layout of the experiment with a time-dependent sequence of concentrations of vapors A and B delivered to the sensing film. For statistics, we included several replicates of exposures to vapors. As illustrative examples, Figure 4A,B depict results of this experiment plotted as film absorbance at 510 and 610 nm, respectively. These figure panels visualize a five-fold difference between the response magnitude of the sensing film to ethyl acetate (vapor A) vs. benzene (vapor B) at 510 nm and almost no difference at 610 nm. Figure 4C,D depict the time-dependent responses of PC_1 and PC_2, respectively from a built PCA model. This multivariate spectral analysis of the film absorbance provided a clear visualization of response differences between individual ethyl acetate and benzene vapors and their mixtures. The PCA model for the binary mixtures involved only a subset of the classification space as compared to the model for six vapors shown in Figure 3B.

Our concept of quantifying individual vapors in their mixtures using a single LSPR film (see Figure 1B) we further demonstrated experimentally as shown in Figure 5. For this analysis, we selected 86 absorption spectra that corresponded to concentrations of individual vapors, their mixtures, and the baseline (see the Supporting Information). The designed map of vapors concentrations (Figure 5A) had an excellent resemblance with the experimentally obtained map (Figure 5B). This data shows the power of the application of 3D networked nanoparticles functionalized with a soft ligand

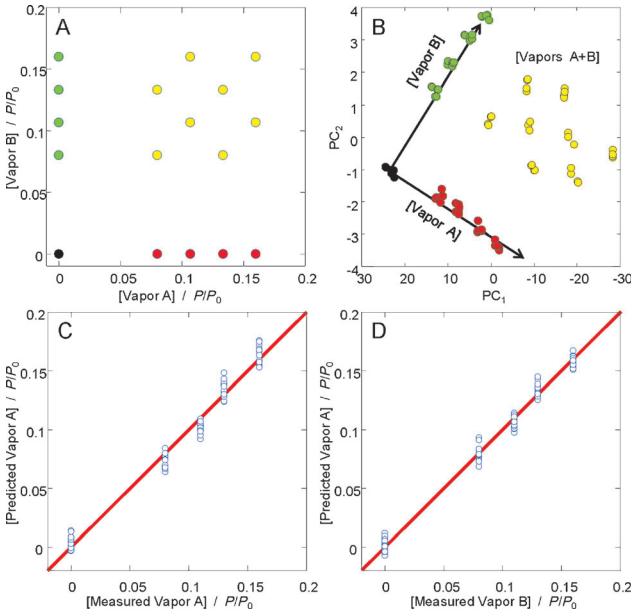

Figure 5. Quantitation of vapors in their binary mixtures using a single sensing film of organothiol-functionalized plasmonic nanoparticles. Comparison between A) a designed map and B) PCA results. Correlation plots between the actual (measured) and predicted cross-validated concentrations of C) ethyl acetate and D) benzene vapors (vapors A and B, respectively). For this quantitation, 86 absorption spectra that corresponded to concentrations of individual vapors, their mixtures, and the baseline were used.

shell for the discrimination of vapors in their binary mixtures. Individual vapors and all their mixtures were clearly resolved.

To quantify vapor concentrations, we applied a multivariate linear regression model using partial least squares (PLS) technique.[14] The PLS technique determines correlations between the independent variables and the instrument response by finding the direction in the multidimensional space of the instrument response that explains the maximum variance for the independent variables. We used PLS to quantify individual vapors in these mixture experiments based on the 86 absorption spectra. From our initial analysis, we selected three latent variables (see Figure S3) that were further used for concentration predictions. The cross-validation of the model was performed using a cross-validation with random samples with five splits and 20 iterations. Figure 5C,D illustrate correlation plots between the actual and predicted cross-validated concentrations of ethyl acetate and benzene vapors. The residual error plots for these vapors are presented in Figure S4. This data illustrates the ability of a single sensing film of organothiol-functionalized gold nanoparticles to not only discriminate but also to quantify individual vapors in their mixtures.

Statistics of quantitation of individual vapors in these mixture experiments is presented in Table S2. The key outputs of the developed multivariate model are the root-mean-square error of calibration (RMSEC) and the root-mean-square error of cross-validation (RMSECV). The prediction accuracy of the developed model was 0.006–0.008 P/P_0. If needed, approaches to improve the accuracy of prediction further could be to develop more robust calibration models based on a larger number of calibration samples and to explore nonlinear multivariate regression models.[17]

Response drift has been reported in organothiol-functionalized nanoparticle films on chemiresistors.[13b,18] We observed the wavelength-dependent baseline drift. It was negligible at 510 nm and noticeable at 610 nm (Figure 2). PC_1 and PC_2 also had different baseline drift (Figure 4C,D). This drift affected the prediction accuracy of concentrations of vapors in their mixtures. To determine the wavelength-dependent baseline drift in more detail, we took the ratio of absorption spectra measured in dry nitrogen before and after exposures to all vapors. This analysis determined the magnitude, direction, and nonmonotonic nature of this drift (Figure S5). While there was no significant drift over 400–500 nm, the drift increased from 500 to 690 nm, stabilized at its maximum at 690 nm, and decreased at longer wavelengths. There could be more than one degradation mechanism of the sensing film,[13b,18] responsible for film instability. The origin of this drift is the focus of our on-going studies.

In conclusion, we showed that a single film of monolayer-functionalized gold nanoparticles coupled with plasmonic readout discriminated between diverse individual vapors and quantified vapors in their simple mixtures. Our vision for multivariable sensing materials for detection of individual vapors and their mixtures introduces a new perspective for sensing, where tunable selectivity is achieved in a single sensing film, rather than from an array of separate sensors. The design requirements to achieve a desired tunable vapor selectivity with such a single film include vapor-induced modulation of the interparticle spacing D through the length of the ligand shell, refractive index of the ligand shell n, reflectivity R of the nanoparticle network film, and their relative contributions to the total mutlivariable response. The number of vapors that could be quantified with such new sensors will be at least two–three, similar to sensor arrays.[19] However, the use of a single sensor simplifies system design, improves sensor stability, and allows new sensor readouts with smartphones and in wearable devices.[20] The present film can quantify individual vapors at most in binary mixtures and could be affected by other vapors. Our current work is focused on enhancing dimensionality of multivariable response of individual sensors, quantifying vapors mixed with interferences, and selectivity tuning by a designed exclusion of sensor response to specific vapors.

Received: June 20, 2013
Published online: August 12, 2013

Keywords: analytical methods · chemoselectivity · nanoparticles · sensors · surface plasmon resonance

[1] a) H. Baltes, J. Hesse, J. G. Korvink, *Sensors Update*, *Vol. 9*, VCH, Weinheim, **2001**; b) J. Fraden, *Handbook of Modern Sensors: Physics, Designs, and Applications*, Springer, New York, **2004**; c) S. Soloman, *Sensors Handbook*, 2nd ed., McGraw-Hill, New York, **2010**.

[2] a) J. Janata, *Principles of Chemical Sensors*, 2nd ed., Springer, New York, **2009**; b) R. A. Potyrailo, R. R. Naik, *Annu. Rev. Mater. Res.* **2013**, *43*, 307.
[3] a) P. C. Jurs, G. A. Bakken, H. E. McClelland, *Chem. Rev.* **2000**, *100*, 2649; b) F. Röck, N. Barsan, U. Weimar, *Chem. Rev.* **2008**, *108*, 705; c) R. A. Potyrailo, V. M. Mirsky, *Chem. Rev.* **2008**, *108*, 770; d) S. E. Stitzel, M. J. Aernecke, D. R. Walt, *Annu. Rev. Biomed. Eng.* **2011**, *13*, 1; e) S. Marco, A. Gutierrez-Galvez, *IEEE Sens. J.* **2012**, *12*, 3189.
[4] K. Persaud, G. Dodd, *Nature* **1982**, *299*, 352.
[5] a) S. H. Lim, L. Feng, J. W. Kemling, C. J. Musto, K. S. Suslick, *Nat. Chem.* **2009**, *1*, 562; b) G. Peng, U. Tisch, O. Adams, M. Hakim, N. Shehada, Y. Y. Broza, S. Billan, R. Abdah-Bortnyak, A. Kuten, H. Haick, *Nat. Nanotechnol.* **2009**, *4*, 669; c) L. D. Bonifacio, G. A. Ozin, A. C. Arsenault, *Small* **2011**, *7*, 3153; d) F. I. Bohrer, E. Covington, C. Kurdak, E. T. Zellers, *Anal. Chem.* **2011**, *83*, 3687; e) K. P. Raymond, I. B. Burgess, M. H. Kinney, M. Lončar, J. Aizenberg, *Lab Chip* **2012**, *12*, 3666.
[6] a) A. Hierlemann, R. Gutierrez-Osuna, *Chem. Rev.* **2008**, *108*, 563; b) R. A. Potyrailo, C. Surman, N. N. Nagraj, A. Burns, *Chem. Rev.* **2011**, *111*, 7315.
[7] a) R. A. Potyrailo, W. G. Morris, *Anal. Chem.* **2007**, *79*, 45; b) R. A. Potyrailo, N. Nagraj, C. Surman, H. Boudries, H. Lai, J. M. Slocik, N. Kelley-Loughnane, R. R. Naik, *TrAC Trends Anal. Chem.* **2012**, *40*, 133; c) B. Li, D. N. Lambeth, *Nano Lett.* **2008**, *8*, 3563; d) S. Rumyantsev, G. Liu, M. S. Shur, R. A. Potyrailo, A. A. Balandin, *Nano Lett.* **2012**, *12*, 2294; e) R. A. Potyrailo, A. M. Leach, C. M. Surman, *ACS Comb. Sci.* **2012**, *14*, 170; f) R. A. Potyrailo, Z. Ding, M. D. Butts, S. E. Genovese, T. Deng, *IEEE Sens. J.* **2008**, *8*, 815; g) R. A. Potyrailo, H. Ghiradella, A. Vertiatchikh, K. Dovidenko, J. R. Cournoyer, E. Olson, *Nat. Photonics* **2007**, *1*, 123; h) B. Rout, L. Unger, G. Armony, M. A. Iron, D. Margulies, *Angew. Chem.* **2012**, *124*, 12645; *Angew. Chem. Int. Ed.* **2012**, *51*, 12477; i) N. A. Joy, M. I. Nandasiri, P. H. Rogers, W. Jiang, T. Varga, S. V. N. T. Kuchibhatla, S. Thevuthasan, M. A. Carpenter, *Anal. Chem.* **2012**, *84*, 5025.
[8] a) C.-S. Cheng, Y.-Q. Chen, C.-J. Lu, *Talanta* **2007**, *73*, 358; b) K.-J. Chen, C.-J. Lu, *Talanta* **2010**, *81*, 1670; c) L. E. Kreno, J. T. Hupp, R. P. Van Duyne, *Anal. Chem.* **2010**, *82*, 8042; d) M. C. Dalfovo, R. C. Salvarezza, F. J. Ibañez, *Anal. Chem.* **2012**, *84*, 4886; e) N. A. Joy, P. H. Rogers, M. I. Nandasiri, S. Thevuthasan, M. A. Carpenter, *Anal. Chem.* **2012**, *84*, 10437.
[9] a) H. Wohltjen, A. W. Snow, *Anal. Chem.* **1998**, *70*, 2856; b) T. E. Mlsna, S. Cemalovic, M. Warburton, S. T. Hobson, D. Mlsna, S. V. Patel, *Sens. Actuators B* **2006**, *116*, 192; c) J. W. Grate, D. A. Nelson, R. Skaggs, *Anal. Chem.* **2003**, *75*, 1868.
[10] C.-L. Li, Y.-F. Chen, M.-H. Liu, C.-J. Lu, *Sens. Actuators B* **2012**, *169*, 349.
[11] a) H.-L. Zhang, S. D. Evans, J. R. Henderson, R. E. Miles, T.-H. Shen, *Nanotechnology* **2002**, *13*, 439; b) W. H. Steinecker, M. P. Rowe, E. T. Zellers, *Anal. Chem.* **2007**, *79*, 4977.
[12] M. Brust, D. Bethell, C. J. Kiely, D. J. Schiffrin, *Langmuir* **1998**, *14*, 5425.
[13] a) F. P. Zamborini, M. C. Leopold, J. F. Hicks, P. J. Kulesza, M. A. Malik, R. W. Murray, *J. Am. Chem. Soc.* **2002**, *124*, 8958; b) Y. Joseph, B. Guse, G. Nelles, *Chem. Mater.* **2009**, *21*, 1670; c) R. A. Potyrailo, C. Surman, M. Pietrzykowski, M. Larsen, *SPIE Photonics West BIOS Conference "Plasmonics in Biology and Medicine VIII"*, *January 23–24*, *2011*, *San Francisco*, *CA* **2011**, Paper 7911.
[14] H. Martens, M. Martens, *Multivariate Analysis of Quality. An Introduction*, Wiley, Chichester, **2001**.
[15] a) P. A. Snow, E. K. Squire, P. S. J. Russell, L. T. Canham, *J. Appl. Phys.* **1999**, *86*, 1781; b) Y. Y. Li, F. Cunin, J. R. Link, T. Gao, R. E. Betts, S. H. Reiver, V. Chin, S. N. Bhatia, M. J. Sailor, *Science* **2003**, *299*, 2045; c) H. Yang, P. Jiang, *Appl. Phys. Lett.* **2011**, *98*, 011104; d) I. B. Burgess, N. Koay, K. P. Raymond, M. Kolle, M. Lončar, J. Aizenberg, *ACS Nano* **2012**, *6*, 1427; e) L. D. Bonifacio, D. P. Puzzo, S. Breslau, B. M. Willey, A. McGeer, G. A. Ozin, *Adv. Mater.* **2010**, *22*, 1351.
[16] a) R. B. Bjorklund, S. Zangooie, H. Arwin, *Appl. Phys. Lett.* **1996**, *69*, 3001; b) A. M. Ruminski, M. M. Moore, M. J. Sailor, *Adv. Funct. Mater.* **2008**, *18*, 3418.
[17] R. A. Potyrailo, R. J. May, T. M. Sivavec, *Sens. Lett.* **2004**, *2*, 31.
[18] a) C. Jin, P. Kurzawski, A. Hierlemann, E. T. Zellers, *Anal. Chem.* **2008**, *80*, 227; b) N. Garg, A. Mohanty, N. Lazarus, L. Schultz, T. R. Rozzi, S. Santhanam, L. Weiss, J. L. Snyder, G. K. Fedder, R. Jin, *Nanotechnology* **2010**, *21*, 405501.
[19] a) M.-D. Hsieh, E. T. Zellers, *Anal. Chem.* **2004**, *76*, 1885; b) C. Jin, E. T. Zellers, *Anal. Chem.* **2008**, *80*, 7283.
[20] a) F. Tsow, E. Forzani, A. Rai, R. Wang, R. Tsui, S. Mastroianni, C. Knobbe, A. J. Gandolfi, N. J. Tao, *IEEE Sens. J.* **2009**, *9*, 1734; b) P. Anzenbacher, Jr., F. Li, M. A. Palacios, *Angew. Chem.* **2012**, *124*, 2395; *Angew. Chem. Int. Ed.* **2012**, *51*, 2345; c) P. Preechaburana, M. C. Gonzalez, A. Suska, D. Filippini, *Angew. Chem.* **2012**, *124*, 11753; *Angew. Chem. Int. Ed.* **2012**, *51*, 11585.

